Anti- and pro-apoptotic activities of baculovirus and *Drosophila* IAPs in an insect cell line

Alex J. Harvey[1], Hatem Soliman[1], William J. Kaiser[1] and Lois K. Miller[1,2,3]

[1] Department of Genetics, The University of Georgia, Athens, Georgia 30602, USA

[2] Department of Entomology, The University of Georgia, Athens, Georgia 30602, USA

[3] corresponding author: Lois K. Miller, tel: (706) 542-2294; fax: (706) 542-2279; e-mail: miller@bscr.uga.edu

Abstract

The anti-apoptotic activities of two baculovirus IAPs, OpIAP and CpIAP, were directly compared with that of two *Drosophila* IAPs, DIAP1 and DIAP2, in the same insect cell line, SF-21 cells. Like OpIAP and CpIAP, DIAP1 inhibited actinomycin D-induced apoptosis and apoptosis induced by Doom. Removal of the RING finger of DIAP1 reduced but did not eliminate its anti-apoptotic activity. DIAP2 was unable to inhibit actinomycin-D induced apoptosis but was able to partially inhibit Doom-induced apoptosis. The baculoviral BIR and RING finger regions, when separated, were unable to block apoptosis induced by actinomycin D or Doom. Instead, the BIR regions of OpIAP and CpIAP as well as the RING finger regions of CpIAP and DIAP1 induced apoptosis. Thus, there were significant differences in the manner in which the different domains of the viral and cellular homologues of IAPs interacted with the components of the pathways regulating apoptosis in SF-21 cells.

Keywords: *iap*; baculovirus; apoptosis; *mod(mdg4)*; Doom; DIAP1

Introduction

Multicellular organisms possess a cellular defense mechanism that results in the directed suicide, known as programmed cell death and/or apoptosis, of cells that may be deleterious to the organism (reviewed by Arends and Wyllie, 1991; Wyllie *et al*, 1980). Cells targeted for apoptosis include those infected with viruses, extra cells formed during development, and cells that have suffered irreparable DNA damage and/or are dividing unchecked (reviewed by Steller, 1995; Thompson, 1995). These cells will actively end their existence by a series of morphological and biochemical processes including proteolysis of specific proteins, cell surface blebbing, breakdown of chromatin structure, and apoptotic body formation.

The obvious importance of apoptosis to cellular biology has led to a search for apoptotic regulatory genes. Disease-linked genetic aberrations, developmental mutations, and viruses have been the source of many apoptotic regulatory genes. Viruses are a particularly rich source of apoptotic regulatory genes because of the need to counteract the host cell apoptotic defense mechanism. Viral apoptotic genes have become invaluable in probing the cellular apoptotic circuitry and identifying cellular homologues or counterparts. The baculoviruses, a family of large DNA-containing insect viruses, have contributed two classes of anti-apoptotic genes, *p35* and the *iap*s. P35, which is encoded by the nuclear polyhedrosis viruses of *Autographa californica* (AcMNPV) and *Bombyx mori* (BmNPV) can block apoptosis induced by a variety of stimuli in insects, mammals, and nematodes (Clem *et al*, 1991; Hay *et al*, 1994; Kamita *et al*, 1993; Rabizadeh *et al*, 1993; Sugimoto *et al*, 1994). P35 binds to and inactivates members of the family of interleukin-1β-converting enzyme (ICE)-like cysteine proteases (Bump *et al*, 1995; Xue and Horvitz, 1995). The ability of P35 to function in many diverse cellular backgrounds has made it an important probe for the detection of ICE-like proteases in uncharacterized apoptotic pathways.

The baculovirus IAPs, Cp-IAP and Op-IAP, were isolated from *Cydia pomonella* granulosis virus (CpGV) and *Orgyia pseudotsugata* nuclear polyhedrosis virus (OpMNPV), respectively (Birnbaum *et al*, 1994; Crook *et al*, 1993). These IAPs were identified by their ability to substitute for P35 in blocking AcMNPV-induced apoptosis in the SF-21 cell line, which is derived from the lepidopteran insect species, *Spodoptera frugiperda*, the fall armyworm. The IAPs have no structural similarity to the P35 protein but instead have two types of zinc-coordinating motifs, the baculovirus IAP repeat (BIR) and a carboxyl-terminal RING finger, both of which are required for anti-apoptotic activity (Clem and Miller, 1994). RING finger motifs are found in a number of proteins involved in such diverse cellular activities as transcription, DNA repair and cell proliferation (reviewed by Freemont, 1993) whereas the BIR motif is unique to IAPs and is tandemly repeated in the amino-terminal and central portions of the protein (reviewed by Clem *et al*, 1996). In addition to blocking baculovirus-induced apoptosis, OpIAP and CpIAP can block actinomycin D-induced apoptosis in SF-21 cells

in the absence of other viral factors, indicating that the IAPs interact directly with cellular apoptotic pathways (Clem and Miller, 1994). The baculovirus IAPs also can inhibit apoptosis in developing *Drosophila* eyes and mammalian cells (Duckett *et al*, 1996; Hay *et al*, 1995; Uren *et al*, 1996).

Humans, mice and *Drosophila* possess cellular IAP homologues which have two or three BIRs and, in most cases, a RING finger at the carboxyl-terminus (Duckett *et al*, 1996; Hay *et al*, 1995; Liston *et al*, 1996; Rothe *et al*, 1995; Roy *et al*, 1995; Uren *et al*, 1996). A *Drosophila* IAP homologue, DIAP1, was identified in a screen for mutations that enhance the effect of *reaper* and *hid*-dependent apoptosis in the developing eye (Hay *et al*, 1995). A second *Drosophila* IAP homologue, DIAP2 (also called DIAP, DILP, or DIHA) was identified by sequence homology (Duckett *et al*, 1996; Hay *et al*, 1995; Liston *et al*, 1996; Uren *et al*, 1996). Ectopic expression of DIAP1 or DIAP2 inhibits *reaper* or *hid*-induced apoptosis in the developing eye. DIAP1 encodes two BIRs and DIAP2 encodes three BIRs and both DIAPs have a carboxyl-terminal RING finger. The full-length DIAP1 inhibits apoptosis in the developing *Drosophila* eye but inhibition is enhanced if the RING finger region is removed from the coding sequence. Expression of the RING finger region alone enhances apoptosis in the developing *Drosophila* eye. Likewise, a human IAP homologue, c-IAP1, is not able to inhibit apoptosis in the developing *Drosophila* eye unless its RING finger region is removed (Hay *et al*, 1995). The neuronal apoptosis inhibitory protein (NAIP), identified as having a possible role in spinal muscular atrophy in humans, lacks a RING finger motif in its coding sequence and blocks apoptosis in mammalian cell lines (Roy *et al*, 1995).

Doom, a *Drosophila* protein which can induce apoptosis in insect cells, was identified by its ability to interact with the baculovirus IAPs (Harvey *et al*, 1996). Doom is encoded by one of five known alternative mRNAs of the *Drosophila mod(mdg4)* gene. *Mod(mdg4)* has been implicated in the regulation of gene expression and chromatin structure but has not yet been linked to the regulation of apoptosis in *Drosophila* (Dorn *et al*, 1993; Gerasimova *et al*, 1995). Doom, when expressed in insect cells, rapidly induces apoptosis which can be blocked by OpIAP, CpIAP and P35 (Harvey *et al*, 1996). The Doom-IAP interaction is mediated through the IAP BIR region (defined as the region encompassing both BIR motifs) and does not require the IAP RING finger. When coexpressed with IAP truncations encoding only the BIR region, Doom can still induce apoptosis. Therefore binding of the BIR region alone to Doom is insufficient to block Doom-induced apoptosis. The BIR region must be physically attached to the RING finger region in order to block Doom-induced apoptosis, suggesting that the IAPs interact with additional, unknown factors through the RING finger region.

The differential dependence of the members of the IAP family on the presence of the RING finger and the structural diversity of the BIR region led us to investigate the individual roles of the BIR and RING finger regions. We compared the influence of the BIR and RING finger regions of DIAP1, DIAP2, and the baculovirus IAPs, OpIAP and CpIAP, on cellular and Doom-induced apoptotic pathways in SF-21 cells. We found that, when separated, the baculovirus BIR and RING finger regions cannot block apoptosis and have an opposite effect, the induction of apoptosis. Removal of the RING finger region from DIAP1 and DIAP2 reduced the anti-apoptotic activity of these proteins, although the BIR region of DIAP1 retained some anti-apoptotic activity.

Results

Construction and expression of IAP truncations

Full length baculovirus and *Drosophila* IAPs were expressed in SF-21 cells under control of the heat-inducible heat shock promoter, HSP70 (Figure 1). The BIR and RING finger regions of OpIAP, CpIAP, and DIAP1 and the BIR region of DIAP2 were manipulated so that they could be expressed separately (Figure 1). Because antibodies to the IAPs are not available, the full-length IAPs and IAP truncations, except for DIAP1-RING, were tagged at the amino-terminus with the hemagglutinin (HA) epitope (designated Epi-tag) to allow detection of expressed proteins (Figure 1).

Attempts to express untagged and tagged DIAP1 from the first methionine of the cDNA sequence were unsuccessful. A DIAP1 construct which was Epi-tagged at the first methionine (Figure 2A) rapidly degraded into small peptides upon expression (data not shown). DIAP1 encodes a second methionine which is at the N-terminus end of the first BIR repeat and is flanked by sequences which fit the consensus for *Drosophila* start codons, suggesting that it can be used as a start codon (Figure 2A). We also noticed that pBSDIAP1-ORF and pGMRDIAP1-BIR (described as pBSDIAP1β-ORF and pGMRDIAP1β-BIR in this paper) provided by B Hay lacked the coding sequence for the first 34 amino acids of the DIAP1 cDNA. Accordingly all untagged DIAP1 and DIAP1-BIR clones used in this paper started from the second methionine and are designated DIAP1β and DIAP1β-BIR (Figure 1). To construct EpiDIAP1β and EpiDIAP1β-BIR, the second methionine was replaced with the HA epitope tag (Figures 1 and 2A). Untagged and Epi-tagged DIAP2s were successfully constructed and expressed using its first methionine (Figure 1).

To express the proteins, the plasmids were transiently transfected into SF-21 cells followed by heat-shock treatment; a procedure which does not induce apoptosis in SF-21 cells transfected with control plasmids (Clem and Miller, 1994). To confirm expression of Epi-tagged proteins, cells transfected with Epi-tagged constructs were harvested at 4 h post-heat shock followed by immunoblot analysis. All Epi-tagged proteins were expressed at detectable levels and migrated at their expected molecular weights during polyacrylamide electrophoresis (Figure 2B and C). Levels of expression were similar for all constructs except for Epi-tagged CpIAP RING (EpiCpR-ING) which was expressed at approximately tenfold lower levels.
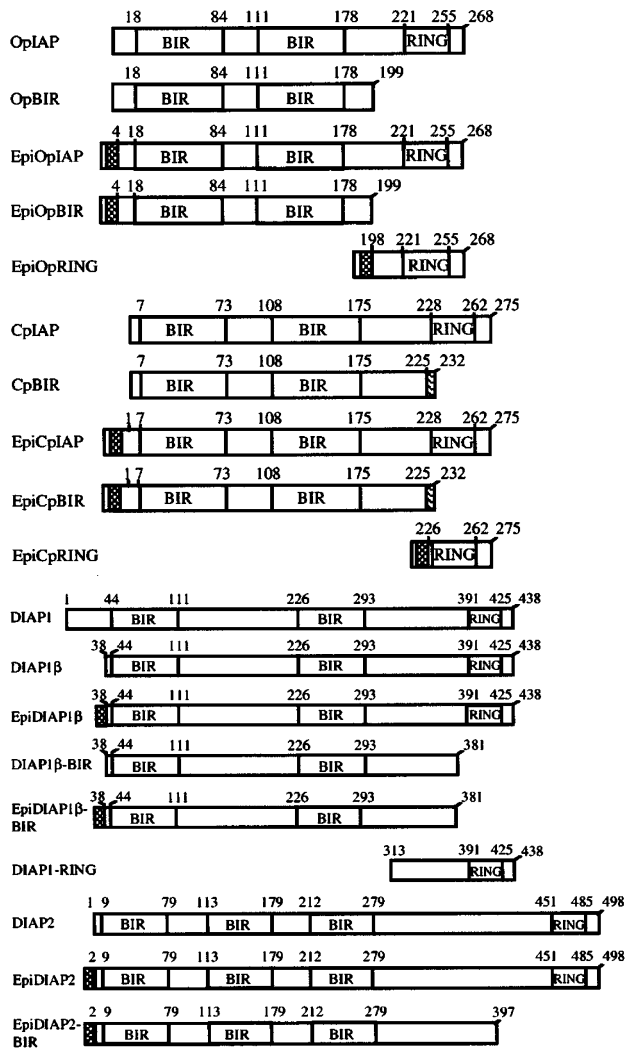
Figure 1 Schematic representations of untagged and Epi-tagged IAPs and their truncations. Numbers indicate amino acid positions relative to the full-length sequences of their open reading frames. The HA epitope tags are denoted by the checkered regions. BIR and RING denotes the baculovirus *iap* repeat and RING finger regions, respectively. The altered reading frame after the frameshift in the CpBIR constructs is denoted by the zig-zag pattern. Note that the scale of the DIAPs is compressed relative to the baculovirus IAPs

Figure 2 Alternate start codons of DIAP1 and expression of Epi-tagged IAPs. (**A**) The sequence of the amino terminus of DIAP1 is shown. The first and second methionines and start codons are in bold. The −4 and −3 positions are single underlined. The start of the first BIR is double underlined. The first arrow indicates the start of the nucleotide sequence of untagged DIAP1β clones. The second arrow indicates the position at which the DIAP1β sequence was fused to the HA epitope tag. (**B**) and (**C**) Expression vectors encoding the indicated proteins were transfected into SF-21 cells. At 4 h post-heat shock, cellular lysates were harvested and analyzed by immunoblot analysis using anti-HA polyclonal antiserum. Positions of Epi-tagged proteins are indicated by the arrows. Positions of molecular weight standards (in kilodaltons) are shown

The BIR and RING finger regions of the baculovirus IAPs do not block actinomycin D-induced apoptosis

The viability of SF-21 cells treated with actinomycin D can be increased by prior transfection with OpIAP and CpIAP-encoding plasmids, confirming the role of IAPs in inhibition of apoptosis (Clem and Miller, 1994). We therefore compared the abilities of the Epi-tagged IAPs and IAP truncations to inhibit apoptosis induced by actinomycin D. To ensure that equivalent amounts of plasmid DNA were used in each transfection, chloramphenicol acetyltransferase (CAT)-expressing plasmids were added to some transfection mixtures. The coexpression of CAT with the IAP proteins had no effect on any of the observed activities
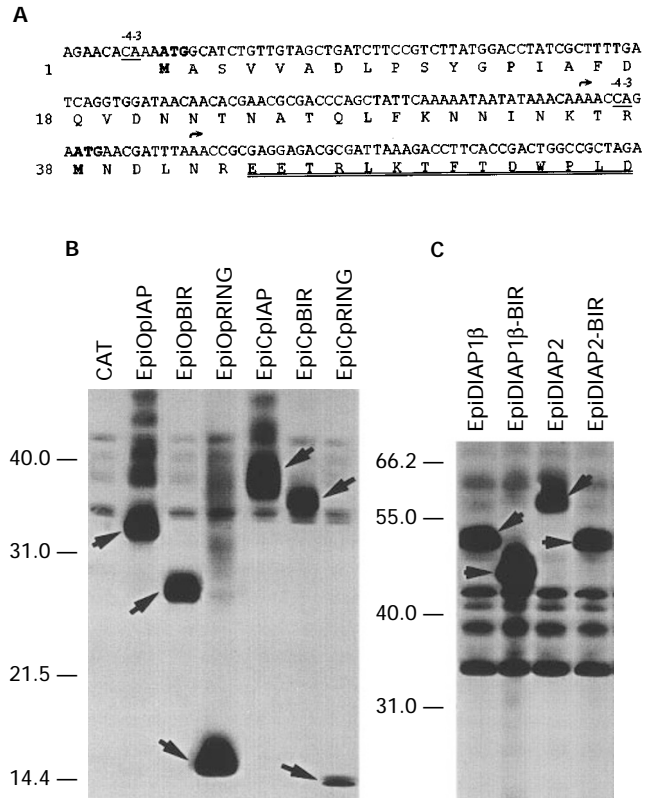
(data not shown). Untagged OpIAP and the Epi-tagged IAPs, EpiOpIAP and EpiCpIAP, inhibited actinomycin D-induced apoptosis at similar levels, indicating that the Epi-tagged IAPs functioned in a comparable manner to untagged OpIAP (Figure 3). The levels of protection are approximately twofold higher than previously described (Clem and Miller, 1994) because of a higher transfection efficiency achieved using lipofectin instead of calcium phosphate during the transfection procedure. Cells expressing Epi-tagged or untagged BIR regions of CpIAP and OpIAP showed no protection against actinomycin D, indicating that the BIR regions alone cannot inhibit apoptosis induced by actinomycin D (Figure 3). Expression of the Epi-tagged RING finger regions of the IAPs also afforded no protection for SF-21 cells treated with actinomycin D (Figure 3). To determine if the BIR and RING finger regions can work when expressed *in trans*, OpBIR and EpiOpRING or CpBIR and EpiCpRING were cotransfected into SF-21 cells. These cells also showed no resistance to induction of apoptosis by actinomycin D,

indicating that the BIR and RING finger regions of the baculovirus IAPs must be covalently linked in order to function (Figure 3).

The BIR region of the baculovirus IAPs induce apoptosis

In the course of these experiments, we noticed that cells expressing the baculovirus BIR regions exhibited cell surface blebbing and apoptotic body formation in the absence of actinomycin D. To confirm the induction of apoptosis by the BIR regions, we assayed for chromatin degradation as indicated by nucleosomal laddering. Both OpBIR and CpBIR, and their Epi-tagged counterparts, induced detectable nucleosomal ladders by 8 h post-heat shock (Figure 4A, left panel). The induction of laddering by tagged BIRs leveled out at 8 h while the laddering induced by untagged BIRs increased up to 24 h, indicating that the epitope tag was interfering with the ability of BIRs to induce apoptosis over an extended period of time (Figure 4A, right panel). This effect could be a result of reduced cellular concentrations of tagged BIRs relative to untagged BIRs either due to decreased expression or protein stability. We cannot compare the cellular levels of tagged and untagged IAPs because our efforts to raise antibodies against the baculovirus IAPs have been unsuccessful. In some experiments, laddering induced by CpBIR at 8 h was more prominent or equal to the intensity of laddering observed at 24 h (Figures 4A and 5A, B).
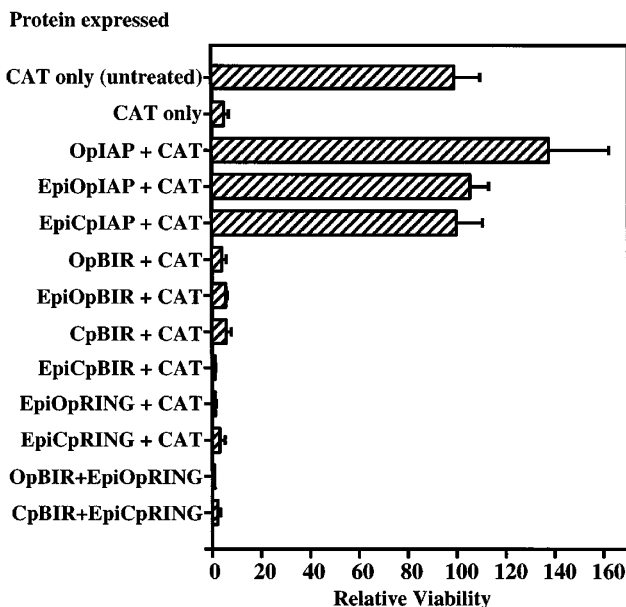

Figure 3 Full-length baculovirus IAPs but not truncations protect against actinomycin D-induced apoptosis. SF-21 cells expressing the indicated proteins were treated with actinomycin D at 4 h post-heat shock. CAT-expressing plasmids were used to balance concentrations of plasmids transfected into cells. Cell viability was determined 20 h later by the trypan blue exclusion assay. Viability was compared to untreated chloramphenicol acetyltransferase (CAT)-transfected cells counted at the time of actinomycin D treatment

Although OpBIR and CpBIR both induced cytopathic effects indicative of apoptosis, there were noticeable differences in the timing and morphology of membrane blebbing. OpBIR and EpiOpBIR induced membrane blebbing which was most prominent at 24 h post-heat shock (Figure 4B, panels 2 and 3). CpBIR induced two distinct morphological changes, both of which were most prominent at 8 to 12 h post-heat shock. Most cells affected by CpBIR displayed membrane blebbing similar to that observed for OpBIR-treated cells (Figure 4B, panel 4). A smaller percentage of CpBIR-transfected cells underwent extensive elongation of the entire cell and did not exhibit any signs of membrane blebbing (Figure 4B, panel 5). Some OpBIR cells also demonstrated elongation but these were far less frequent than that observed for CpBIR (data not shown). EpiCpBIR-transfected cells behaved like CpBIR-transfected cells except that the cytopathic effects were most prominent at 24 h post-heat shock (Figure 4B, panel 6).

BIR-induced cell death was not widespread until 24 h after heat shock induction, at which time unaffected cells had divided and obscured the reduction in cell number. Therefore counts of viable cells as determined by the trypan blue assay did not accurately reflect the extent of apoptosis observed by visible membrane blebbing and nucleosomal laddering. To obtain a quantitative estimate of BIR-induced apoptosis, the percentage of cells demonstrating blebbing and elongation was determined at 8 and 24 h post-heat shock by microscopic inspection. OpBIR and EpiOpBIR induced blebbing in 60% and 20% of cells remaining at 24 h post-heat shock, respectively (Figure 4C). CpBIR and EpiCpBIR induced apoptosis in 30% and 15% of cells remaining at 8 h post-heat shock, respectively (Figure 4C). CpBIR blebbing was reduced to 15% of remaining cells at 24 h post-heat shock, presumably because most CpBIR-transfected cells had completely disintegrated at that time.

Full-length IAPs and P35 can inhibit BIR-induced apoptosis

To further confirm that the cellular changes induced by the BIRs are indicative of apoptosis, the ability of full-length IAPs and P35 to inhibit BIR-induced apoptosis was tested. At 8 h post-heat shock both P35 and the IAPs were able to block OpBIR and CpBIR-induced apoptosis as judged by the nucleosomal ladder assay (Figure 5A). P35 and the IAPs were also able to block BIR-induced membrane blebbing and cell elongation (data not shown). Cotransfection of the RING finger constructs with the BIR constructs had no effect or slightly increased the extent of apoptosis (Figure 5A and B). CpIAP blocked OpBIR-induced apoptosis and OpIAP blocked CpBIR-induced apoptosis (Figure 5A).

At 24 h post-heat shock, BIR-induced apoptosis was still completely blocked by P35 but the ability of the IAPs to block BIR-induced apoptosis was significantly reduced (Figure 5B). OpIAP partially inhibited OpBIR and CpBIR-induced apoptosis while CpIAP was totally ineffective at 24 h post-heat shock. Western analysis indicated that the cellular concentrations of the Epi-tagged IAPs at 24 h had
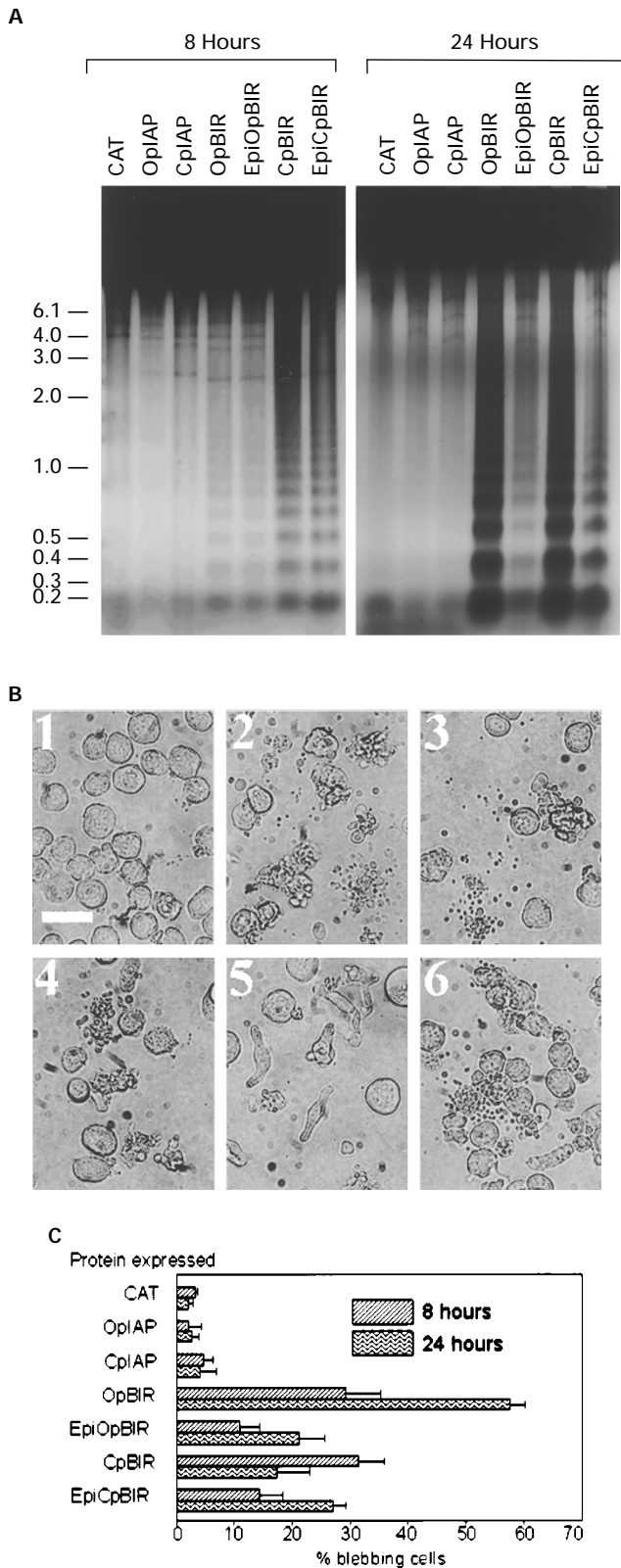
A

8 Hours   24 Hours

CAT, OpIAP, CpIAP, OpBIR, EpiOpBIR, CpBIR, EpiCpBIR

6.1 —
4.0 —
3.0 —
2.0 —
1.0 —
0.5 —
0.4 —
0.3 —
0.2 —

B

C

Protein expressed

CAT
OpIAP
CpIAP
OpBIR
EpiOpBIR
CpBIR
EpiCpBIR

8 hours
24 hours

0   10   20   30   40   50   60   70
% blebbing cells

Figure 4 Baculovirus BIRs induce apoptosis. (**A**) SF-21 cells were transfected with plasmids expressing the protein indicated above each lane under heat shock promoter control. Cellular DNA was harvested at 8 and 24 h post-heat shock, separated by agarose gel electrophoresis, stained with ethidium bromide and visualized on a fluorimager. Positions of molecular weight standards (in kilobases) are shown. (**B**) SF-21 cells were heat shocked at t=0 h following cotransfection with plasmids expressing the following proteins under heat shock promoter control. Photographs were taken at the indicated times post-heat shock: chloramphenicol acetyltransferase (CAT), 24 h (panel 1); OpBIR plus CAT, 24 h (panel 2); EpiOpBIR plus CAT, 24 h (panel 3); CpBIR plus CAT, 8 h, two different fields (panels 4 and 5); EpiCpBIR plus CAT, 24 h (panel 6); Scale bar 25 μm. (**C**) The percentage of cells demonstrating blebbing and elongation induced by expression of the indicated constructs was determined at 8 and 24 h post-heat shock as described in Materials and Methods

declined to approximately 10% of the levels observed at 4 and 8 h post-heat shock whereas the concentration of Epi-tagged P35 at 24 h was reduced to 50% of the levels observed at 8 h post-heat shock (Figure 5C). Therefore, due to either differences in expression or stability, the cellular levels of P35 during the experiment were more uniform than OpIAP or CpIAP and could account for its ability to provide long-term protection against BIR-induced apoptosis. Although we were not able to compare the influence of the epitope tag on cellular concentrations of IAPs because antiserum specific to the IAPs was not available, untagged and tagged IAPs both protected at 8 h but not at 24 h, suggesting that the epitope tag did not affect the expression or stability of the IAPs. P35 also did not seem to be affected by the epitope tag as tagged and untagged P35 protected as well at 24 h post-heat shock (data not shown).

CpRING induces apoptosis

Transfection of EpiCpRING into SF-21 cells induced nucleosomal laddering that was detectable at 24 h post-heat shock (Figure 6A). EpiCpRING induced both membrane blebbing and cell elongation similar to that observed for CpBIR (Figure 6B, panel 3). EpiCpRING-induced cytopathic effects were visible in approximately 25% of the cells present at 24 h post-heat shock (Figure 6C). EpiOpRING did not induce any signs of apoptosis (Figure 6A and B, panel 2). The EpiOpRING construct used encoded an extra 20 amino acids not present in EpiCpRING (Figure 1), therefore we created a second EpiOpRING construct which was more similar in size to EpiCpRING. The second EpiOpRING construct also did not induce any signs of apoptosis (data not shown) indicating the extra 20 amino acids was not responsible for lack of EpiOpRING activity.

The ability of P35 and full-length IAPs to block EpiCpRING-induced apoptosis was similar to that de-scribed for BIR-induced apoptosis. While at 8 h EpiCp-RING-induced nucleosomal laddering was barely detectable, some EpiCpRING-induced cytopathic effects were visible except in cells cotransfected with P35 or CpIAP (data not shown). At 24 h post-heat shock, EpiCpRING-induced laddering and blebbing was signifi-cantly reduced by P35 (Figure 6A and C). CpIAP had no effect on EpiCpRING-induced laddering (Figure 6A) and reduced blebbing moderately (Figure 6C).

DIAP1-RING induces apoptosis and DIAP1β partially inhibits actinomycin D-induced apoptosis

Expression of full-length DIAP1β or DIAP1β-BIR did not produce any signs of apoptosis while DIAP1-RING induced both nucleosomal laddering (Figure 7A) and membrane blebbing (data not shown). DIAP1β-BIR was able to partially inhibit DIAP1-RING-induced apoptosis (Figure 7A). Full-length DIAP2 and Epi-tagged DIAP2-BIR, EpiDIAP2-BIR, did not produce signs of apoptosis in SF-21 cells (data not shown). The RING finger region of DIAP2 was not expressed separately in this study.

The DIAP1β and DIAP2 constructs were tested for their ability to inhibit actinomycin D-induced apoptosis. DIAP1β protected 30% of SF-21 cells from actinomycin D-induced apoptosis (Figure 7B). Other constructs, including the untagged or tagged DIAP1β-BIR, untagged and tagged full-length DIAP2, and tagged DIAP2-BIR, showed marginal levels of protection that were not significantly above the background protection afforded by expression of CAT (Figure 7B). EpiDIAP1β did not protect against actinomycin D-induced apoptosis as determined by counting of trypan-blue stained cells 20 h after addition of actinomycin D (Figure 7B) but some protection was observed in cells at 4 or 8 h (data
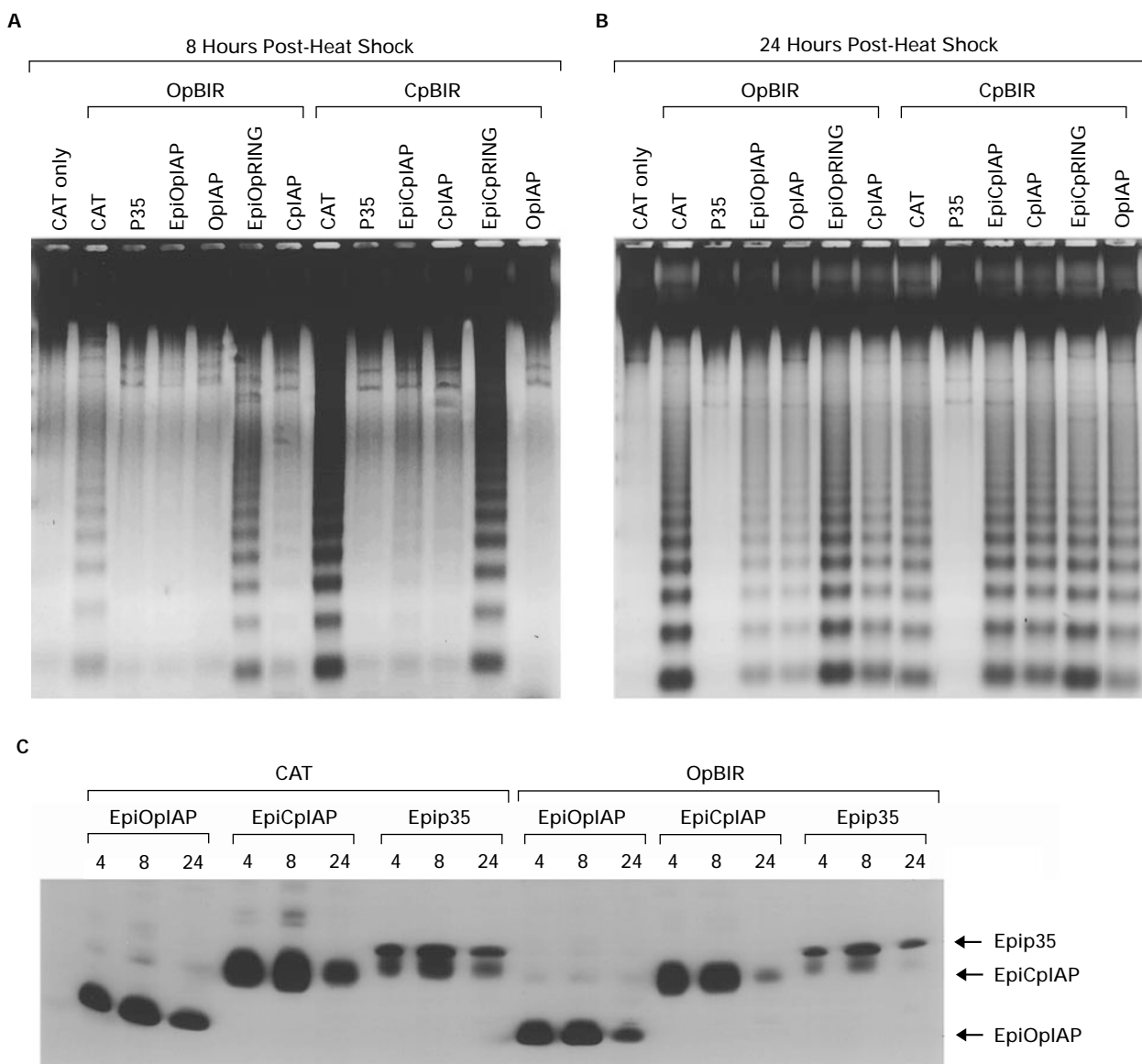

Figure 5 Inhibition of BIR-induced apoptosis by p35 and full-length IAPs. (**A**) and (**B**) SF-21 cells were transfected with plasmids expressing the protein(s) indicated above each lane under heat shock promoter control. Cellular DNA was harvested at 8 (**A**) and 24 (**B**) h post-heat shock, separated by agarose gel electrophoresis, stained with ethidium bromide and visualized on a fluorimager. (**C**) SF-21 cells coexpressing CAT or OpBIR with EpiOpIAP, EpiCpIAP or Epip35 were harvested at 4, 8 and 24 h post-heat shock. Cellular lysates were analyzed by immunoblot analysis using anti-HA polyclonal antiserum. Positions of Epi-tagged proteins are indicated by the arrows
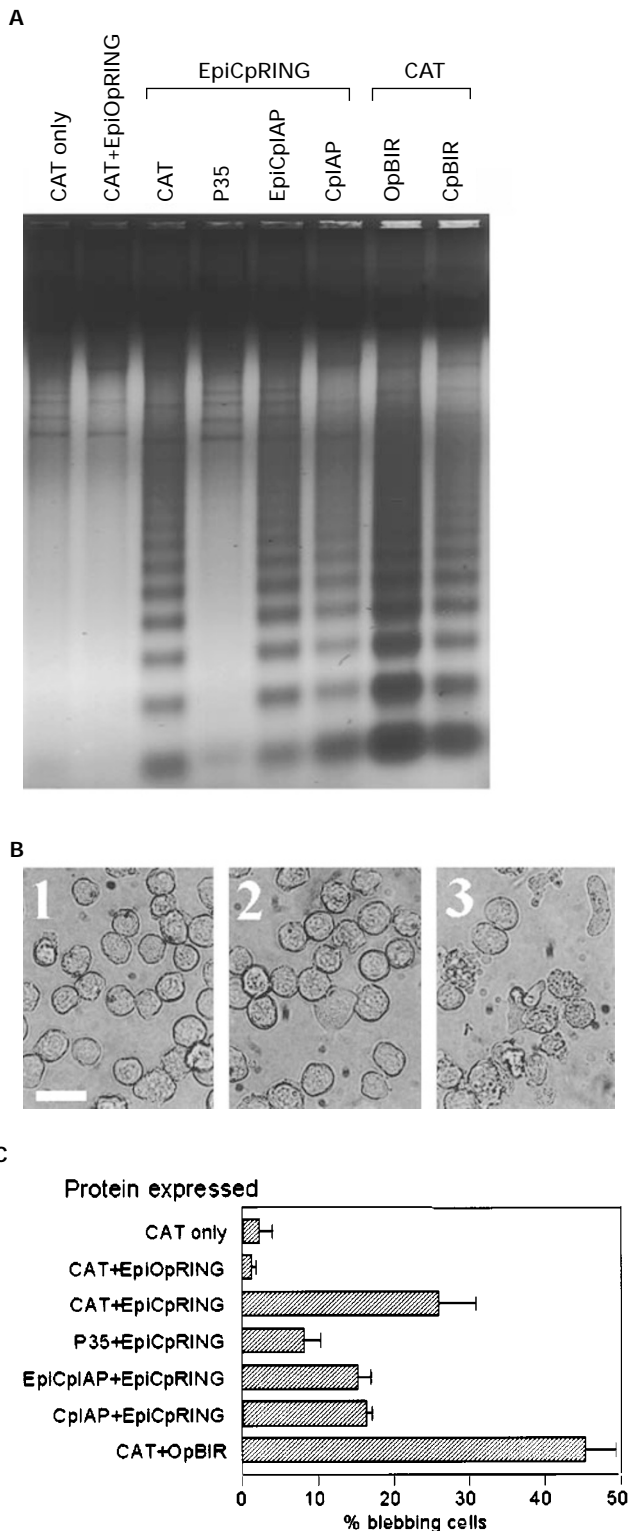
Figure 6 The RING finger region of CpIAP but not OpIAP induces apoptosis. (**A**) SF-21 cells were transfected with plasmids expressing the protein(s) indicated above each lane under heat shock promoter control. Cellular DNA was harvested at 24 h post-heat shock, separated by agarose gel electrophoresis, stained with ethidium bromide and visualized on a fluorimager. (**B**) SF-21 cells were heat shocked at t=0 h following cotransfection with plasmids expressing the following proteins under heat shock promoter control. Photographs were taken at 24 h post-heat shock:

chloramphenical acetyltransferase (CAT), (panel 1); EpiOpRING plus CAT, (panel 2); EpiCpRING plus CAT, (panel 3); Scale bar 25 μm. (**C**) The percentage of cells demonstrating blebbing and elongation induced by expression of the indicated constructs was determined at 24 h post-heat shock as described in Materials and Methods

not shown). Thus, the epitope tag interfered with the anti-apoptotic activity of DIAP1β in actinomycin D-treated cells.

Baculovirus and *Drosophila* IAPs can inhibit Doom-induced apoptosis

The entire Doom open reading frame was fused to the FLAG epitope, creating FlagDoom (also called FlagDoom(1–514) (Harvey *et al*, 1996)). Within 3 h post-heat shock, FlagDoom induced membrane blebbing and, at 8 h post-heat shock, nucleosomal laddering and extensive membrane blebbing was apparent (Figures 8A and 9), as described for FlagDoom (99–514) (Harvey *et al*, 1996). As previously described, full length baculovirus IAPs blocked FlagDoom-induced apoptosis as judged by the extent of laddering detected at 8 h post-heat shock (Figure 8A) (Harvey *et al*, 1996). The baculovirus BIR and RING finger regions, transfected alone or together, were not able to block FlagDoom-induced apoptosis (Figure 8A).

DIAP1β and EpiDIAP1β inhibited FlagDoom-induced apoptosis at 8 h post-heat shock as indicated by the reduction in nucleosomal laddering (Figure 8B) and membrane blebbing (Figure 9). DIAP1β-BIR slowed but did not block FlagDoom-induced apoptosis as nucleosomal laddering was evident at 8 h (Figure 8B) and membrane blebbing was widespread by 8 h post-heat shock (Figure 9). EpiDIAP1β-BIR had little effect on FlagDoom-induced apoptosis as laddering was marginally reduced (Figure 8B) and there was no effect on blebbing (data not shown). EpiDIAP1β and EpiDIAP1β-BIR were detected at similar levels when coexpressed with FlagDoom (data not shown), indicating that removal of the RING finger did not effect the expression or stability of the DIAP1 constructs. DIAP1-RING did not inhibit FlagDoom-induced apoptosis nor did DIAP1-RING alter the inhibitory effect of DIAP1-BIR (Figure 8B).

EpiDIAP2 but not untagged DIAP2 marginally reduced nucleosomal laddering induced by FlagDoom (Figure 8B) but both DIAP2 and EpiDIAP2 significantly reduced membrane blebbing at 8 h post-heat shock (Figure 9, data not shown for DIAP2). EpiDIAP2-BIR had no effect on FlagDoom-induced nucleosomal laddering and membrane blebbing (Figures 8B and 9). Both EpiDIAP2 and EpiDIAP2-BIR were difficult to detect in cells expressing FlagDoom (data not shown), indicating that these proteins were unstable in the apoptotic environment.

Discussion

Whereas full-length baculovirus IAPs block actinomycin D- and Doom-induced apoptosis, the BIR and RING finger regions did not block actinomycin D or Doom-induced apoptosis when expressed alone or coexpressed *in trans*, indicating that the BIR and RING finger regions of these viral

A

IAPs must be covalently attached in order to block apoptosis (see Table 1 for a summary of the results). Although the BIR regions of the baculovirus IAPs physically interact with Doom (Harvey *et al*, 1996), the apoptotic activity of Doom was not reduced when coexpressed with BIRs alone or with the BIRs and RING finger. The interpretation of these data are complicated by the unexpected observation that expression of the baculovirus BIRs alone induced apoptosis in SF-21 cells. The BIRs may be inducing apoptosis by displacing endogenous cellular IAPs, thereby disrupting their anti-apoptotic function; the lack of the RING finger may disrupt normal signaling exerted by endogenous IAPs.

DIAP1β was able to inhibit actinomycin D and Doom-induced apoptosis, confirming its anti-apoptotic behavior. Removal of the RING finger from DIAP1β significantly reduced but did not abolish its anti-apoptotic activity, indicating that, as previously reported, the BIR region of DIAP1 can act to inhibit apoptosis (Hay *et al*, 1995). However, in the developing *Drosophila* eye, DIAP1-BIR is significantly more active than DIAP1, suggesting that the RING finger is acting as a negative regulator of DIAP1 activity (Hay *et al*, 1995). In SF-21 cells, removal of the RING finger from DIAP1β abolished its ability to block actinomycin D-induced apoptosis and reduced its ability to block Doom-induced apoptosis.

The difference in behavior of the DIAP1 RING finger region may be a result of the heterologous nature of the SF-21 cell assay system. The behavior of an exogenous protein in SF-
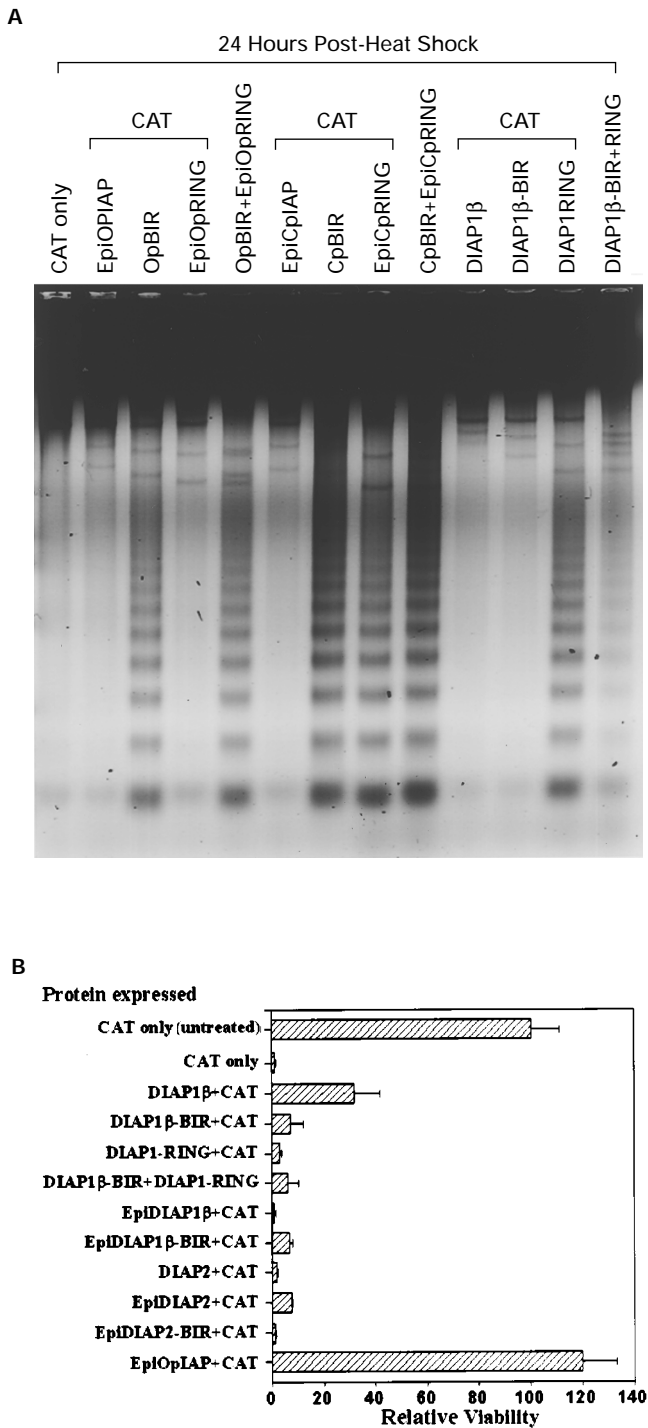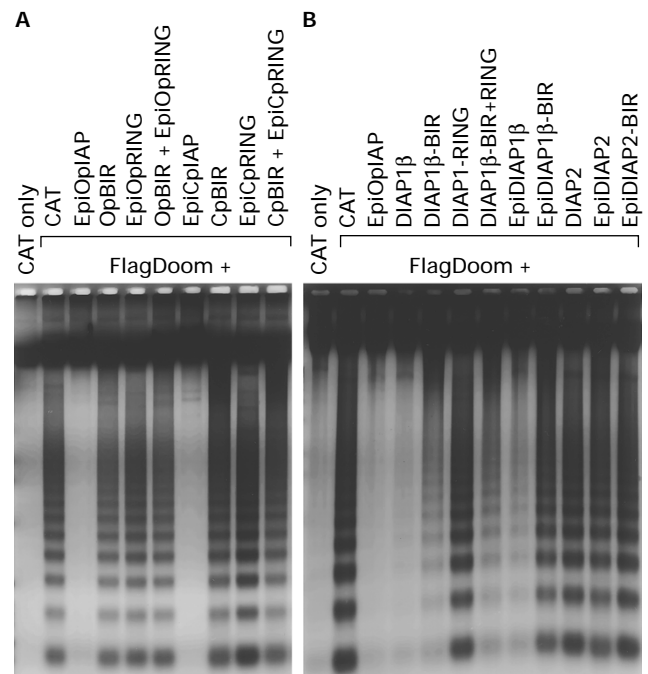
B

Figure 7 The RING finger region of DIAP1 induced apoptosis and DIAP1β inhibited actinomycin D-induced apoptosis. (**A**) SF-21 cells were transfected with plasmids expressing the protein(s) indicated above each lane under heat shock promoter control. CAT-expressing plasmids were used to balance concentrations of plasmids transfected into cells. Cellular DNA was harvested at 24 h post-heat shock, separated by agarose gel electrophoresis, stained with ethidium bromide and visualized on a fluorimager. (**B**) SF-21 cells expressing the indicated proteins were treated with actinomycin D at 4 h post-heat shock. Cell viability was determined 20 h later by the trypan blue exclusion assay. Viability was compared to untreated CAT-expressing cells counted at the time of actinomycin D treatment

A   **B**

Figure 8 Inhibition of Doom-induced chromatin degradation by baculovirus and *Drosophila* IAPs. (**A**) and (**B**) SF-21 cells were transfected with plasmids expressing the protein(s) indicated above each lane under heat shock promoter control. CAT-expressing plasmids were used to balance concentrations of plasmids transfected into cells. Cellular DNA was harvested at 8 h post-heat shock, separated by agarose gel electrophoresis, stained with ethidium bromide and visualized on a fluorimager

21 cells may differ from that in the cell lineage or species in which it is normally expressed. An additional consideration is that we were unable to express DIAP1 from its first methionine, as any expressed protein was rapidly degraded. Both full-length DIAP1 (translated from the first methionine) and a truncated form of DIAP1 lacking the RING finger were rapidly degraded into small peptides and

CAT only

FlagDoom + CAT

FlagDoom + DIAP1β

FlagDoom + DIAP1β-BIR

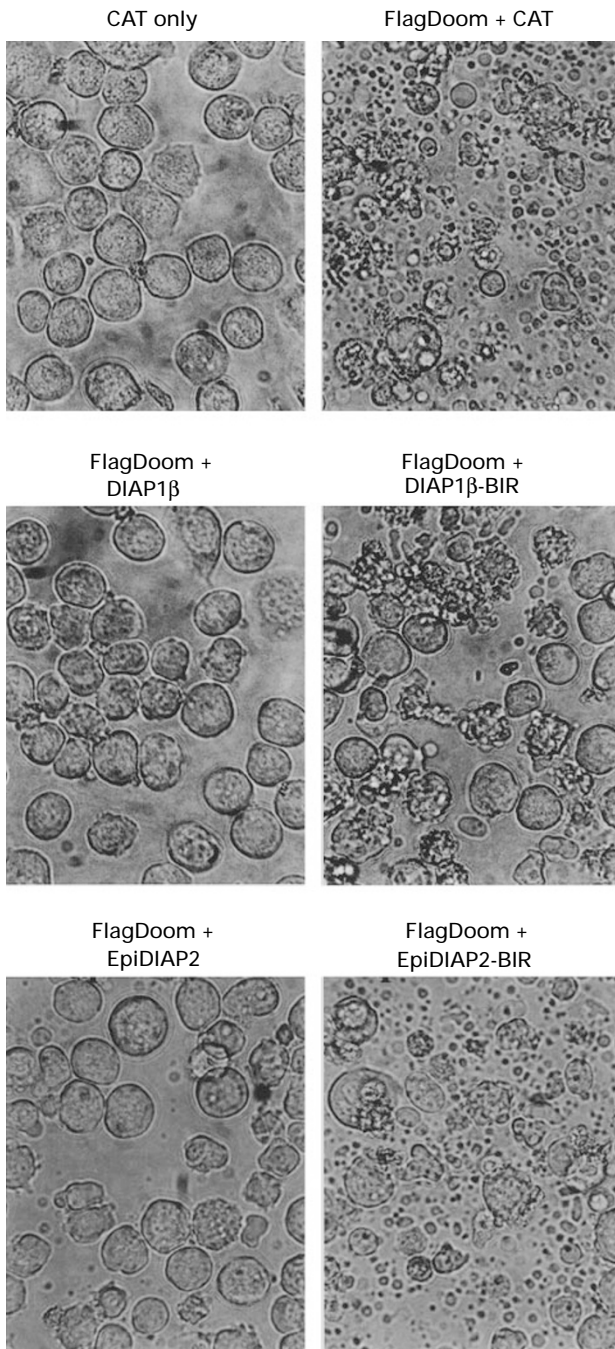FlagDoom + EpiDIAP2

FlagDoom + EpiDIAP2-BIR

Figure 9 Inhibition of Doom-induced membrane blebbing by *Drosophila* IAPs. SF-21 cells were transfected with plasmids expressing the protein(s) indicated above each photograph under heat shock promoter control. CAT-expressing plasmids were used to balance concentrations of plasmids transfected into cells. Photographs were taken at 8 h post-heat shock

demonstrated no anti- or pro-apoptotic activity (data not shown). The possibility exists that full-length DIAP1 would be more stable in *Drosophila* and behave differently; more information is needed regarding the behavior of the full-length and truncated forms of DIAP1 in the context of *Drosophila* cells.

Epi-tagged DIAP2 was able to inhibit FlagDoom-induced membrane blebbing but not nucleosomal laddering. In cells induced to undergo apoptosis by FlagDoom, membrane blebbing emerges at 2 – 3 h post-heat shock while significant chromatin degradation is not detectable until 8 h post-heat shock (Harvey *et al*, 1996). When FlagDoom was coexpressed with EpiDIAP2, nucleosomal laddering was reduced only slightly at 8 h post-heat shock. Membrane blebbing was delayed and was not evident until 8 h, at which time it was greatly reduced as compared to cells expressing FlagDoom alone. It is likely that these differences were due to the low levels of EpiDIAP2 in the presence of FlagDoom. We had difficulty detecting EpiDIAP2 (and EpiDIAP2-BIR) in cells expressing FlagDoom, presumably due to instability of DIAP2 in the SF-21 apoptotic environment (data not shown). The level of EpiDIAP2 may not be sufficient to inhibit FlagDoom-induced nucleosomal laddering but be sufficient to inhibit FlagDoom-induced membrane blebbing. The low EpiDIAP2 expression in the SF-21 apoptotic environment is consistent with the observed lack of protection against actinomycin D-induced apoptosis; inhibition of actinomycin D-induced apoptosis may require higher levels of protein expression.

The RING finger regions of CpIAP and DIAP1 also induced apoptosis when expressed separately from the BIR region. It is unknown why the RING finger truncation of OpIAP did not behave similarly because the amino acid 219 – 268 region of OpIAP, which includes the RING finger, is 58% and 56% identical to the corresponding regions of DIAP1 and CpIAP, respectively. In addition, a functional hybrid IAP can be created by replacing the RING finger of CpIAP with the RING finger of OpIAP, indicating that the RING finger regions of OpIAP and CpIAP are interchangeable (Clem and Miller, 1994). However, the region encompassing amino acids 226 – 275 of CpIAP is 70% identical to the corresponding region of DIAP1 but only 56% identical to OpIAP, suggesting that the RING fingers of CpIAP and DIAP1 are more similar in secondary and tertiary structure than that of OpIAP and may function optimally in different apoptotic pathways. The variation in the behavior of the RING fingers may reflect the ability of the RING fingers to function in different pathways in the cell. The fact that none of the IAPs tested have evolved specifically to function in SF-21 cells (although they can block apoptosis in this cell line) makes interpretation of these specific effects difficult.

AcMNPV carries two IAP homologues, AcIAP1 and AcIAP2, which apparently are not sufficient to block viral-induced apoptosis in SF-21 cells as P35 mutant viruses rapidly undergo apoptosis upon infection of SF-21 cells (Ayres *et al*, 1994; Braunagel *et al*, 1992; Clem *et al*, 1991; Clem and Miller, 1993). OpMNPV carries four IAP homologues (Ahrens *et al*, 1997; Birnbaum *et al*, 1994). While OpIAP, also called OpIAP-3, has been shown to be an apoptotic inhibitor (Birnbaum *et al*, 1994), the role of the

Table 1 Apoptotic activities of baculovirus and *Drosophila* IAPs in SF-21 cells

		Inhibited		
IAP Domain	Induced apoptosis	Actinomycin D-induced apoptosis	Doom-induced chromatin degradation	Doom-induced membrane blebbing
CpIAP and OpIAP				
Full[a]	No[e]	Yes[d]	Yes	Yes
BIRs[b]	Yes	No	No	No
RING[c]	Yes[f]	No	No	No
DIAP1β				
Full	No	Yes[g]	Yes	Yes
BIRs	No	No	Yes[g]	Yes[g]
RING	Yes	No	No	No
DIAP2				
Full	No	No	No	Yes[g]
BIRs	No	No	No	No
RING	ND[h]	ND	ND	ND

[a]Full, full-length IAP. [b]BIRs, region containing two or three BIR motifs. [c]RING, RING finger domain. [d]Yes indicates that either the untagged or Epi-tagged or both versions of the domain demonstrated activity. [e]No indicates that no activity was observed for the untagged and Epi-tagged versions of each domain. [f]The RING finger of OpIAP did not induce apoptosis. [g]Inhibition of apoptosis was not complete or partial. [h]ND, not determined

additional viral IAPs remains to be determined. It is possible that these viruses encode multiple IAPs so that a variety of apoptotic signaling pathways can be silenced, thus increasing the host and/or tissue range of the virus. Likewise baculovirus IAPs have maximized their protective abilities by coevolution of the BIRs and RINGs. It is unlikely that the RING finger plays a regulatory role in the viral life cycle; it would not be advantageous for the virus to downregulate its anti-apoptotic response. Thus during the evolution of baculoviruses, they have retained the IAP RING finger region to enhance protection against the cellular apoptotic response.

Analogous to the baculoviruses, the presence of multiple IAP homologues in higher eukaryotes suggests that those proteins may have evolved somewhat different functions so that they function optimally in different apoptotic signaling pathways. Although most have been shown to inhibit apoptosis to varying degress, the actual physiological role of these IAPs remains to be established. The eukaryotic IAPs possibly have evolved to regulate a variety of biological activities, including cell fate and cell cycle. The BIRs and RINGs would have evolved so that the anti-apoptotic activity is regulated and not constitutive. Thus for at least some cellular IAPs, the BIRs and RINGs would have evolved independently such that the BIR is anti-apoptotic while the RING counters the activity of the BIR. The balance between the activities of the BIRs and RINGs of eukaryotes could depend on the cellular environment and the availability of interacting factors that reside in one or more apoptotic pathways. As the cellular targets of the BIRs and RINGs are determined, the role and regulation of the IAPs should become clearer.

Materials and Methods

Expression plasmid construction

To construct pHSEpiOpIAP*Nru*I, the OpIAP open reading frame in pHSOpIAP*Nru*I (described in Clem and Miller, 1994) was epitope-tagged at the amino-terminal *Ava*I site by insertion of DNA encoding the sequence RYPYDVPDYARA. The sequence YPYDVPDYA constitutes the hemagglutinin epitope, HA.11. pHSEpiOpIAPdel was created by deleting the *Pml*I – *Pml*I fragment, which overlaps the RING finger domain, creating a frameshift starting at amino acid 249 of OpIAP and continuing an additional 27 amino acids. pHSEpiOpBIR and pHSOpBIR was created by deleting from pHSEpiOpIAP*Nru*I and pHSOpIAP*Nru*I, respectively, the region between the *Nru*I site at amino acid 199 and the *Cla*I site in the 3′ untranslated region of OpIAP, thereby creating a stop codon after amino acid 199. pHSEpiOpRING was constructed by deleting from pHSEpiOpIAP*Nru*I the region between the *Apa*I site, which resides at the 3′ end of the HA epitope tag, and *Nru*I at amino acid 198, fusing amino acid 198 in frame to the HA epitope tag. pHSepiOpRING2, which encodes a smaller EpiOpRING, was constructed by PCR amplifying a region of pHSOpIAP*Nru*I using the oligo 5′-TCCCCCCGGGGCCCGG-CTGTGCAAGATTTGCC-3′ and the T3 oligo followed by digestion with *Sma*I and *Cla*I. The resulting PCR fragment, which contains a *Sma*I site at the 5′ end of the RING finger coding region and a *Cla*I site at the 3′ end of the 3′ untranslated region, was used to replace the *Sma*I – *Cla*I region of pHSEpiOpIAP*Nru*I.

pHSEpiCpIAP was created by replacing the entire coding region and 3′ untranslated region of pHSEpiOpIAP*Nru*I downstream of the epitope tag with the entire coding region and 3′ untranslated region of CpIAP derived from pHSCpIAP (described in Clem and Miller, 1994). pHSCpBIR and pHSEpiCpBIR were created by cutting pHSCpIAP and pHSEpiCpIAP, respectively, with *Bst*BI, blunt ending with Klenow and religating the linear vectors. pHSEpiCpRING was constructed by cutting pHSCpIAP with *Bst*BI, blunt ending with Klenow, and cutting with *Pst*I. The resulting fragment, which contains the RING finger and 3′ untranslated region of CpIAP was used to replace the coding region and 3′ untranslated region of OpIAP in pHSEpiOpIAP*Nru*I.

pHSEpip35 was constructed by cutting pHSp35VI+ (described in Clem and Miller, 1994) with *Pst*I and *Eco*RI, removing the 5′ and 3′ overhangs, and blunt-end ligating into pHSEpiOpIAP*Nru*I digested with *Sma*I and *Cla*I. The modified *Pst*I end of p35 is in frame with the HA epitope tag and the p35 coding sequence replaces that of OpIAP.

pGMR-DIAP1β-ORF was constructed by inserting the *Eco*RI/filled-in *Not*I fragment of pBSDIAP1β-ORF (which contains nucleotides 534 – 1741 of the DIAP1 cDNA (Hay *et al*, 1995) into the *Eco*RI/*Stu*I site of pGMR. pHSDIAP1β was constructed by inserting the *Hind*III/

*Eco*RI fragment from pGMR-DIAP1β-ORF containing the DIAP1 ORF starting from the second methionine and the HSP70 3′ untranslated region in the *Bgl*II site of pHSP70PL. pHSDIAP1β-BIR was constructed by inserting the *Hind*III/*Eco*RI fragment from pGMRDIAP1β-BIR containing the DIAP1-BIR coding region (starting at nucleotide 534 and ending at 1576 of the DIAP1 cDNA (Hay *et al*, 1995) and the HSP70 3′ untranslated region into the *Bgl*II site of pHSP70PL. pHSDIAP1-RING was constructed by inserting the *Hind*III/*Eco*RI fragment from pGMRDIAP1-RING containing the DIAP1-RING finger coding region and the HSP70 3′untranslated region into the *Bgl*II site of pHSP70PL.

pHSEpiDIAP1β-BIR was constructed by replacing the *Apa*I/*Pml*I region of pHSEpiOpIAP*Nru*I containing the OpIAP ORF and part of the HSP70 3′ untranslated region with the *Dra*I fragment of pHSDIAP1β-BIR, which contains nucleotides 551–1576 of the DIAP1 cDNA and part of the HSP70 3′ untranslated region, so that the DIAP1 ORF is in frame with the HA epitope tag. pHSEpiDIAP1β was constructed by replacing the *Cla*I/*Pst*I region of pHSEpiDIAP1β-BIR with the *Cla*I/*Pst*I region of pGMR-DIAP1β-ORF so that the Epi-tagged DIAP1-ORF has an intact RING finger and a HSP70 3′ untranslated region.

pHSDIAP2 was constructed by inserting the *Eco*RI fragment of pBSDIAP2-ORF, containing the DIAP2 ORF, into the *Bgl*II site of pHSP70. pHSEpiDIAP2 was constructed by PCR of pBSDIAP2-ORF using the oligo 5′-CGCGGATCCCCCGGGTGACGGAG-CTGGGCCTGGAGCTGG-3′ and the T7 oligo followed by digestion with *Sma*I and *Not*I. The resulting PCR fragment, which contains a *Sma*I site at the 5′ end of the DIAP2 coding region and a filled-in *Not*I site at the 3′ end, was used to replace the *Sma*I–*Pml*I region of pHSEpiOpIAP*Nru*I. pHSEpiDIAP2-BIR was constructed by inserting a *Xba*I amber codon linker (New England Biolabs) at the *Age*I site (amino acid 397) of pHSEpiDIAP2.

pHSFlagDoom was constructed by PCR of pBSDoom1 (Harvey *et al*, 1996) using the oligo 5′-CGCGGATCCCCCGGGCGGACGAC-GAGCAATTC-3′ and the T7 oligo followed by digestion with *Sma*I and *Dra*I. The resulting PCR fragment, which contains a *Sma*I site at the 5′ end of the Doom coding region and a *Dra*I site at the 3′ end of the 3′ untranslated region, was used to replace the *Sma*I–*Pml*I region of pHSEpiOpIAP*Nru*I.

Cell culture and transfections

S. frugiperda (fall armyworm) IPLB-SF-21 (SF-21) cells (Vaughn *et al*, 1977) were maintained as previously described (O'Reilly *et al*, 1992). Transfections were carried out as previously described (O'Reilly *et al*, 1992), except transfections were performed on 0.5×10^6 SF-21 cells in 35 mm tissue culture plates and the transfection mixture consisted of 2.5 μl of lipofectin (Gibco-BRL) and 1.0 μg of each plasmid in 0.5 mls incomplete TC-100. After transfection, plates were incubated 20 h at 27°C. Plates were heat shocked as previously described (Clem and Miller, 1994).

Microphotography and quantitation of apoptosis

Phase contrast photography of transfected cells was performed on an Olympus IX50 inverted microsope equipped with a PM-10AK camera. For actinomycin D experiments, the percent of cells undergoing apoptosis was performed as previously described (Clem and Miller, 1994) except cells were transfected using lipofectin and the final concentration of actinomycin D was 500 ng/ml. Note that the actual number of viable cells was increased approximately twofold due to an artifact involving an increased sensitivity of non-actinomycin D-treated cells to scraping, as previously described (Clem and Miller, 1994). To determine the percent of cells undergoing apoptosis at 8 and 24 h post-heat shock due to BIR or RING expression, photographs were taken at the indicated times of three separate transfections. The percentage of cells undergoing apoptosis for a given photograph was determined by counting the number of cells that displayed membrane blebbing and/or elongation and dividing by the total number of cells in the photograph.

Nucleosomal ladder preparation

For nucleosomal ladder preparation, 0.5×10^6 transfected SF-21 cells in 35 mm tissue culture plates were harvested at 8 or 24 h post-heat shock by scraping into the medium. Cells were pelleted at $2000 \times g$ and resuspended in 0.4 M Tris-Cl, pH 7.5, 0.1 M EDTA, then SDS and proteinase K were added to a final concentration of 0.1% and 200 μg/ml, respectively. After 12–20 h at room temperature, lysates were extracted once with phenol/chloroform/isoamyl alcohol (25:24:1) and precipitated with 2.5 volumes of ethanol and 0.1 volumes of 5 M NaCl. After centrifugation at $12\,000 \times g$, DNA pellets were washed with 70% ethanol, dried and resuspended in 30 μl 10 mM Tris-acetate, pH 8.0, 1 mM EDTA, 20 μg/ml RNase A, 0.025% bromophenol blue, 3.0% glycerol. A 1.2% agarose gel was partially submerged in 0.04 M Tris-acetate, pH 8.2, 1 mM EDTA, and wells were half-filled with running buffer. 20 μl of each DNA sample was loaded, electrophoresed at 5 volts/cm for 15 min, the gel was submerged in running buffer and electrophoreses was continued for 2 h. The gel was stained in 20 μg/ml ethidium bromide and visualized on a Molecular Dynamics Fluorimager with no filter.

Immunoblotting

Transfected cells were harvested at 4 h post-heat shock and pelleted at $500 \times g$. Cells were lysed in 50 μl of 0.5 M Tris-Cl, pH 6.8, 10% SDS, 10% glycerol, 1.43 M 2-mercaptoethanol, 0.001% bromophenol blue. 10 μl of total cell lysates were heated to 95°C for 5 min, separated on 12% SDS–PAGE and transferred to Immobilon P membranes (Millipore). Epi-tagged constructs were detected with 1:10 000 dilution of rabbit anti-HA.11 polyclonal antisera (Berkeley Antibody Co.) and 1:20 000 dilution of goat anti-rabbit IgG HRP conjugate (Promega). Immunoblots were visualized with the Enhanced Chemiluminescence (ECL) Western Blotting System (Amersham).

Acknowledgements

References

Ahrens CA, Russell RR, Funk CJ, Evans J, Harwood S and Rohrmann GF (1997) The sequence of the *Orgyia pseudotsugata* multinucleocapsid nuclear polyhedrosis virus genome. Virology 229: 381–399

Arends MJ and Wyllie AH (1991) Apoptosis: mechanisms and role in pathology. Int. Rev. Exp. Pathol. 32: 223–254

Ayres MD, Howard SC, Kuzio J, Lopez-Ferber M and Possee RD (1994) The complete DNA sequence of *Autographa californica* nuclear polyhedrosis virus. Virology 202: 586–605

Birnbaum MJ, Clem RJ and Miller LK (1994) An apoptosis-inhibiting gene from a nuclear polyhedrosis virus encoding a polypeptide with Cys/His sequence motifs. J. Virol. 68: 2521–2528

Braunagel SC, Daniel KD, Reilly LM, Guarino LA, Hong T and Summers MD (1992) Sequence, genomic organization of the EcoRI-A fragment of *Autographa californica* nuclear polyhedrosis virus, and identification of a viral-encoded protein resembling the outer capsid protein VP8 of rotavirus. Virology 191: 1003 – 1008

Bump NJ, Hackett M, Hugunin M, Seshagiri S, Brady K, Chen P, Ferenz C, Franklin S, Ghayur T, Li P *et al* (1995) Inhibition of ICE family proteases by baculovirus antiapoptotic protein p35. Science 269: 1885 – 1888

Clem RJ, Fechheimer M and Miller LK (1991) Prevention of apoptosis by a baculovirus gene during infection of insect cells. Science 254: 1388 – 1390

Clem RJ, Hardwick JM and Miller LK (1996) Anti-apoptotic genes of baculoviruses. Cell Death Differ. 3: 9 – 16

Clem RJ and Miller LK (1993) Apoptosis reduces both the *in vitro* replication and the *in vivo* infectivity of a baculovirus. J. Virol. 67: 3730 – 3738

Clem RJ and Miller LK (1994) Control of programmed cell death by the baculovirus genes *p35* and *iap*. Mol. Cell. Biol. 14: 5212 – 5222

Crook NE, Clem RJ and Miller LK (1993) An apoptosis-inhibiting baculovirus gene with a zinc finger-like motif. J. Virol. 67: 2168 – 2174

Dorn R, Krauss V, Reuter G and Saumweber H (1993) The enhancer of position-effect variegation of *Drosophila, E(var)3-93D*, codes for a chromatin protein containing a conserved domain common to several transcriptional regulators. Proc. Natl. Acad. Sci. USA. 90: 11376 – 11380

Duckett CS, Nava VE, Gedrich RW, Clem RJ, Van Dongen JL, Gilfillan MC, Shiels H, Hardwick JM and Thompson CB (1996) A conserved family of cellular genes related to the baculovirus *iap* gene and encoding apoptosis inhibitors. EMBO J. 15: 2685 – 2694

Freemont PS (1993) The RING finger: a novel protein sequence motif related to the zinc finger. Ann. NY Acad. Sci. 684: 174 – 192

Gerasimova TI, Gdula DA, Gerasimov DV, Simonova O and Corces VG (1995) A *Drosophila* protein that imparts directionality on a chromatin insulator is an enhancer of position-effect variegation. Cell 82: 587 – 597

Harvey AJ, Bidwai AP and Miller LK (1996) Doom, a product of the *Drosophila mod(mdg4)* gene, induces apoptosis and binds to baculovirus inhibitor of apoptosis proteins. In Press

Hay BA, Wassarman DA and Rubin GM (1995) *Drosophila* homologs of baculovirus inhibitor of apoptosis proteins function to block cell death. Cell 83: 1253 – 1262

Hay BA, Wolff T and Rubin GM (1994) Expression of baculovirus P35 prevents cell death in *Drosophila*. Development 120: 2121 – 2129

Kamita SG, Majima K and Maeda S (1993) Identification and characterization of the *p35* gene of *Bombyx mori* nuclear polyhedrosis virus that prevents virus-induced apoptosis. J. Virol. 67: 455 – 463

Liston P, Roy N, Tamai K, Lefebvre C, Baird S, Cherton-Horvat G, Farahani R, McLean M, Ikeda JE, MacKenzie A and Korneluk RG (1996) Suppression of apoptosis in mammalian cells by NAIP and a related family of IAP genes. Nature 379: 349 – 353.

O'Reilly DR, Miller LK and Luckow VA (1992) Baculovirus expression vectors: a laboratory manual. New York: W.H. Freeman & Co.

Rabizadeh S, LaCount DJ, Friesen PD and Bredesen DE (1993) Expression of baculovirus *p35* gene inhibits mammalian neural cell death. J. Neurochem. 61: 2318 – 2321

Rothe M, Pan MG, Henzel WJ, Ayres TM and Goeddel DV (1995) The TNFR2-TRAF signaling complex contains two novel proteins related to baculoviral inhibitor of apoptosis proteins. Cell 83: 1243 – 1252

Roy N, Mahadevan MS, McLean M, Shutler G, Yaraghi Z, Farahani R, Baird S, Besner-Johnston A, Lefebvre C, Kang X *et al* (1995) The gene for neuronal apoptosis inhibitory protein is partially deleted in individuals with spinal muscular atrophy. Cell 80: 167 – 178

Steller H (1995) Mechanisms and genes of cellular suicide. Science 267: 1445 – 1449

Sugimoto A, Friesen PD and Rothman JH (1994) Baculovirus *p35* prevents developmentally programmed cell death and rescues a *ced-9* mutant in the nematode *Caenorhabditis elegans*. EMBO J. 13: 2023 – 2028

Thompson CB (1995) Apoptosis in the pathogenesis and treatment of disease. Science 267: 1456 – 1462

Uren AG, Pakusch M, Hawkins CJ, Puls KL and Vaux DL (1996) Cloning and expression of apoptosis inhibitory protein homologs that function to inhibit apoptosis and/or bind tumor necrosis factor receptor-associated factors. Proc. Natl. Acad. Sci. USA. 93: 4974 – 4978

Vaughn JL, Goodwin RH, Tompkins GJ and McCawley P (1977) The establishment of two cell lines from the insect *Spodoptera frugiperda* (Lepidoptera; Noctuidae). In Vitro. 13: 213 – 217

Wyllie AH, Kerr JFR and Currie AR (1980) Cell death: the significance of apoptosis. Int. Rev. Cytol. 68: 251 – 306

Xue D and Horvitz HR (1995) Inhibition of the *Caenorhabditis elegans* cell-death protease CED-3 by a CED-3 cleavage site in baculovirus p35 protein. Nature 377: 248 – 251